Available online at www.sciencedirect.com
ScienceDirect
Journal of the European Ceramic Society 30 (2010) 1717–1724
www.elsevier.com/locate/jeurceramsoc

Synthesis and characterization of the crystalline powders on the basis of Lu_2O_3:Eu^{3+}spherical submicron-sized particles

Nadya A. Dulina, Yulia V. Yermolayeva*, Alexander V. Tolmachev, Zoya P. Sergienko, Oleh M. Vovk, Elena A. Vovk, Neonilla A. Matveevskaya, Pavel V. Mateychenko

Institute for Single Crystals, NAS of Ukraine, Lenin Ave., 60, 61001 Kharkov, Ukraine

Received 28 August 2009; received in revised form 30 December 2009; accepted 10 January 2010
Available online 4 February 2010

Abstract

This study is devoted to the preparation of the crystalline powders on the basis of non-agglomerated monodisperse Lu_2O_3:Eu^{3+} spherical particles with the diameters in the range of 50–250 nm by the soft chemistry co-precipitation route. The influence of the synthesis parameters on control morphology, particles size and agglomeration in the final Lu_2O_3:Eu^{3+} powder was considered. Lu_2O_3:Eu^{3+} crystalline powders were characterized by means of electron microscopy methods (TEM, SEM), FT-IR spectroscopy, thermal analysis (TG-DTA) and X-ray diffractometry. The mechanisms of the precursor decomposition and crystallization at the temperatures ranging from 60 to 900 °C were discussed. It was shown that the powders obtained were characterized by the effective luminescence under X-ray excitation in $\lambda = 575$–725 nm spectral region corresponding to $^5D_0 \rightarrow {}^7F_J$ transitions ($J = 0$–4) of Eu^{3+} ions with a maximum at 612 nm and the luminescence intensity strongly depends on annealing temperature. The relative densities of the green-bodies on the basis of Lu_2O_3:Eu^{3+} powders were estimated and the sintering of compacts at the temperatures up to 1500 °C was studied.

Keywords: Powders-chemical preparation; Thermal treatment; Electron microscopy; Luminescence; Lu_2O_3:Eu^{3+}

1. Introduction

Currently, crystalline powders on the basis of nano- and submicron-sized spherical luminescent particles are intensively studied due to the possibility of their easy packing into close-density optical materials for high-resolution display technologies, advanced ceramic creation for laser industry and medical detectors.[1–3] High optical quality of ceramics is necessary for all fields of the functional application and substantially provided by the highest possible density of the particles packing (the lowest volume of interparticle voids) at the green-body formation stage. The shape, sizes and degree of the agglomeration of the particles are the main factors which influence on appearance of the defects in compacts, such as pores and heterogeneities, result in density reduction, light dispersion and decrease of ceramics transparency. The usage of the spherical uniform-sized non-agglomerated particles is known to promote the uniform packing of the particles in the green-body with the density up to 70%. At the same time, the density of green-body obtained on the basis of non-spherical particles is generally not higher than 40–45%.[4] The grain boundary mobility and the sintering ability increase for the compacts based on submicron-sized particles as compared with the compacts of micrometric particles. The optimal range of diameters is 70–150 nm, since the smaller particles will be strongly subjected to agglomeration during synthesis because of its extremely high surface energy.[5] It is also possible to enhance the density of the compacts by incorporation of the smaller than the compact-forming particles into the interparticle voids. Therefore, the spherical shape of the particles, homogeneity of their sizes, small degree of agglomeration and possibility to control the diameter of particles for preparation of the fractions with the defined diameter are the most substantial requirements to powders which are used for high-density materials creation.

Presently, a variety of methods have been successfully applied to the preparation of crystalline powders for ceramics, including plasma spraying, chemical co-precipitation, hydrothermal synthesis,[6,7] mechanosynthesis, combustion

* Corresponding author.
E-mail address: yu.yermolayeva@gmail.com (Y.V. Yermolayeva).

0955-2219/$ – see front matter © 2010 Elsevier Ltd. All rights reserved.
doi:10.1016/j.jeurceramsoc.2010.01.019

synthesis procedure with urea fuel, etc.[8–10] Among the mentioned methods, low cost soft chemistry co-precipitation route from water solutions attract much attention due to its simplicity, ecological compatibility and possibility to control the shape and the sizes of particles at high level, and also providing narrow size distribution of the particles.[11,12] Recently the powders on the basis of spherical particles of the compositions Y_2O_3:Eu^{3+}, Gd_2O_3:Eu^{3+}, $(Y_{1-x}Gd_x)_2O_3$:Eu^{3+}, HfO_2:Tb^{3+}, etc. with the given diameters have been obtained by the chemical co-precipitation procedure,[1,13–15] some of their structural and luminescent properties have been studied. However, the assortment of the compounds which obtained in the form of spherical particles is rather limited now. Therewith, the adaptation of the particles obtained to the compaction processes for the preparation of the dense packing on their basis with high quality is desired. For that purposes, it is necessary to add the technological stages, such as specific drying,[16] mechanical milling, which are determined the final morphological parameters of the powder. Currently these aspects are described not enough in the literature.

Lutetium oxide (Lu_2O_3) doped with trivalent europium (Eu^{3+}) ions is a structural analog of effective commercial Y_2O_3:Eu^{3+} red phosphor, and belongs to cubic structure, space group Ia3. Lu_2O_3:Eu^{3+} is one of the most perspective material for X-ray detection and imaging due to high effective atomic number $Z_{eff.} = 67$ and its extremely high density ($\rho = 9.4\ g/cm^3$) in comparison with Y_2O_3 ($\rho = 4.8\ g/cm^3$) and Gd_2O_3 ($\rho = 7.6\ g/cm^3$).[17–19] It is reported earlier that lutetium is more favorable cation than yttrium for lanthanide dopant emission.[20] Nowadays, numerous studies is known devoted to transparent ceramics creation on the basis of Eu^{3+}-doped lutetium oxide with the non-spherical morphology.[21,22] The large light yield of Lu_2O_3:Eu^{3+} ceramics under X-ray excitation (90,000 photon/MeV) was achieved, which 10 times exceeds the light yield of commercial $Bi_4Ge_3O_{12}$ (BGO) single crystals.[23] Application of the submicron-sized Lu_2O_3:Eu^{3+} spherical particles allows one to increase the density of the green-body and as a result reduced the temperatures of green-body densification upon sintering.

Therefore, the main purpose of the present study is preparing of the crystalline powders based on Lu_2O_3:Eu^{3+} spherical particles of a narrow size distribution by the soft chemistry co-precipitation process, analyzing of the influence of the preparing parameters, drying conditions and annealing temperature on the Lu_2O_3:Eu^{3+} crystalline powder morphology and agglomeration.

2. Experimental procedures

Crystalline Lu_2O_3:Eu^{3+} powders have been obtained by the soft chemistry co-precipitation method from the water solutions with subsequent annealing for powders crystallization. Initially, high-purity lutetium oxide (Lu_2O_3, 99.99%) and europium oxide (Eu_2O_3, 99.99%) powders were dissolved in nitric acid to form $Lu(NO_3)_3$ and $Eu(NO_3)_3$ solutions. Ammonium bicarbonate (NH_4HCO_3), ammonium hydroxide (NH_4OH) and urea ($(NH_2)_2CO$) have been used as a precipitants. In the case of synthesis with the NH_4HCO_3 and NH_4OH precipitants, the powder precursor was prepared by the adding of the precipitants water solutions ($0.01\ mol\ L^{-1}$) to a mixture of $Lu(NO_3)_3$ ($0.5\ mol\ L^{-1}$) and $Eu(NO_3)_3$ solutions at a speed of $1\ mL\ min^{-1}$ under mild stirring at room temperature. In the case of urea, synthesis procedure was carried out in water solution, which contains $Lu(NO_3)_3$ ($0.5\ mol\ L^{-1}$), $Eu(NO_3)_3$ and urea ($(NH_2)_2CO$). The molar ratio [Lu^{3+}]/urea varied from 1×10^{-4} to 6×10^{-3}. The mixture was heated at certain temperatures (80–100 °C) to decompose the urea and stirred during 5 h. Europium content was 5 at.% with respect to lutetium in all experiments. Completion of the reaction was established by the pH value of the reactive mixture. The resulting suspension aged during 24 h and then the amorphous precursor was separated by centrifugation or filtration, washed several times with deionized water and ethanol, and dried in air at certain temperatures (25–120 °C). In some experiments the azeotropic dehydration was used for samples drying. The powders obtained was crushed and annealed at 700, 900, 1200 °C in air for 2 h.

The morphology of the samples obtained were studied by means of scanning electron microscopy (SEM) using a JSM-6390 LV (JEOL, Japan) and a transmission electron microscopy (TEM) using a EM-125 (Selmi, Ukraine). Fourier transform infrared spectroscopy (FT-IR) spectra of the samples were measured on a FT-IR spectrometer SPECTRUM ONE (PerkinElmer) with the KBr pellet technique. The X-ray diffraction (XRD) of the powder samples was examined on a DRON-2.0 diffractometer (Fe Kα radiation, λ = 1.93728 Å). The thermal analysis (TG-DTA) were conducted using a MOM Q-1500 derivatograph in air within a temperature interval 20–1000 °C at heating rate of $10\ °C\ min^{-1}$. Brunauer–Emmett–Teller (BET, NOVA 2200, Quantachrome Corp., USA) method with nitrogen as the adsorption molecules at the temperature of liquid nitrogen boiling point (78 K) was used for the specific surface area measuring of the powders obtained.

The X-ray luminescence spectra were obtained using SDL-2 (LOMO, Russia) automated complex. Luminescence was excited by REIS-E X-ray source (Cu-anticathode, deceleration radiation with the energy $E \sim 30\ keV$), operating at $U = 30\ kV$ and $I = 50\ mkA$.

Lu_2O_3:Eu^{3+} powders were compacted into pellets of 10-mm-diameter by means of dry uniaxial pressure method at the pressure ranging from 40 to 440 MPa. The density of the samples was determined by hydrostatic weighing method. The powders densification was carried out using a NETZSCH-402ED differential dilatometer in air within a temperature interval 20–1500 °C at heating rate of the $10\ °C\ min^{-1}$.

3. Results and discussion

Soft chemistry co-precipitation technique has been proved to be feasible for preparation of ceramic powders with favorable characteristics. Close attention is paid to the initial stages of the co-precipitation process of the precursor because the crystalline powders after heat treatment in most cases present the same morphological properties of precursor. It is known that

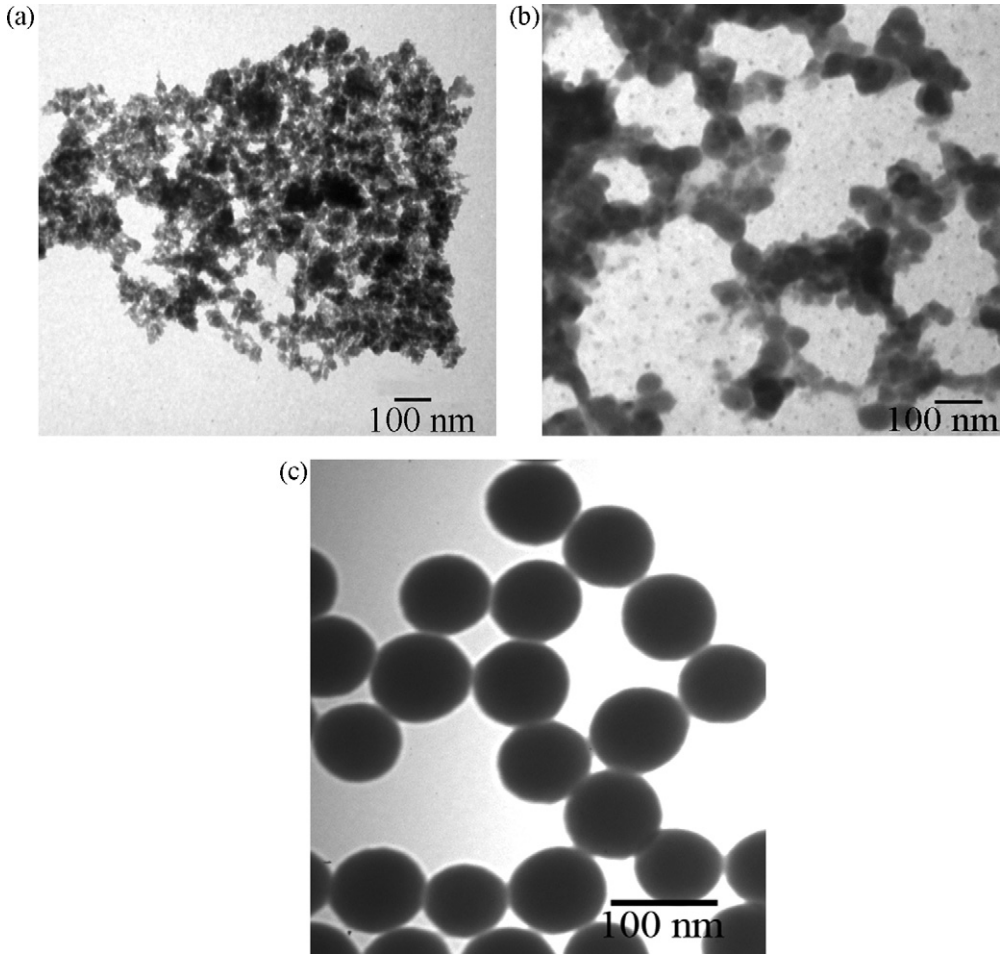

Fig. 1. TEM images of the precipitate precursors prepared with NH_4OH (a), NH_4HCO_3 (b), and $(NH_2)_2CO$ (c) as the precipitants.

the shape, sizes and agglomeration of the precursor particles prepared strongly depend on the co-precipitation parameters, such as precipitant type, concentration of the reagents and temperature. Influence of the different precipitants (NH_4OH, NH_4HCO_3, $(NH_2)_2CO$) on morphology of the Lu_2O_3:Eu^{3+} powders obtained was analyzed. Fig. 1 shows the TEM picture of the precursor powders prepared using different precipitants during co-precipitation.

It is clearly seen, that using ammonia NH_4OH as precipitant results in formation of the strongly agglomerated particles of the non-defined shape with the average size is about 15 nm (Fig. 1a). Such behavior can be explained by high reaction rate causing fast growing rate and uncontrolled severe agglomeration of the resulting particles. The considerably low hydrolysis rate of ammonium bicarbonate NH_4HCO_3 and urea $(NH_2)_2CO$ leads to more homogeneous precipitation process. Application of the NH_4HCO_3 precipitant provides formation of the spherical-like particles with the average diameter of 40 nm (Fig. 1b), however the particles prepared in such way are also strongly agglomerated. Severe agglomeration of the powders precipitated by NH_4OH and NH_4HCO_3 can be explained by the hydrogen bonding of surface hydroxyl groups on the hydroxide and hydroxycarbonate precipitated particles, and also bridging the surface hydroxyl groups of neighboring particles by the water molecules.[23,24] It was established that the uniform-sized non-agglomerated spherical particles were formed in case of urea-based precipitation (Fig. 1c) due to the slow decomposition of urea at the temperature above 80 °C. Urea serves as a reservoir of precipitating anions in this process. Namely, in situ decomposition of urea releases precipitating ligands (OH^- and CO_3^{2-}) slowly and homogeneously into the reaction system avoiding localized distribution of the reactants and, consequently, making control of nucleation and growth possible.[14] The particles are not agglomerated practically because of the relative high synthesis temperature that provides additional thermal agitation in the reaction mixture and promotes destruction of the bonds between particles.

FT-IR spectra measured for the Lu_2O_3:Eu^{3+} precursor prepared using the different precipitants and dried at 40 °C in air are shown in Fig. 2. All FT-IR spectra have the absorption bands near 3435 and 1632 cm^{-1}, which were assigned to stretching vibration and bending vibration of O–H bonds, respectively. Two intense bands at 1530 and 1403 cm^{-1} are observed in all spectra, which are concerned with the asymmetric stretch of C–O in CO_3^{2-} groups. The absorption bands at 1092 and 840 cm^{-1} are assigned as symmetric stretch of C–O band and deformation vibration of C–O in CO_3^{2-} groups, respectively.[23] These absorption bands indicate the presence of carbonate groups

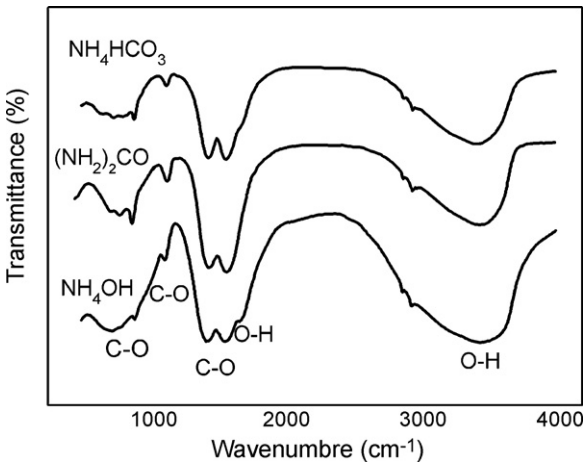

Fig. 2. FT-IR spectra of the precursors prepared using the different precipitants (dried at 40 °C in air).

(CO_3^{2-}) which is caused both by formation of carbonate during the synthesis and absorption of carbon dioxide from the air during the samples drying. Thus, the lutetium basic carbonate $Lu(OH)CO_3{\cdot}H_2O$ precursor was precipitated after the synthesis with the precipitants mentioned above. It was concluded that only urea precipitation leads to the formation of the $Lu(OH)CO_3{\cdot}H_2O$ precursor particles with the desired morphology, that is why urea was used in the further experiments in this study.

The effects of the molar ratio $[Lu^{3+}]$/urea and temperature on the resulting particle diameter were studied in detail (Fig. 3). The influence of the temperature on the particles diameter was shown in Fig. 3a. The bottom limit of the temperature interval was determined by the temperature of the urea decomposition. It is clearly seen that the diameter of particles increased with the rising of the temperature above 90 °C, probably due to the acceleration of formative unit's movement and nucleation rates alteration.

The diameters of Lu_2O_3:Eu^{3+} precursor particles depending on the molar ratio $[Lu^{3+}]$/urea are shown in Fig. 3b. The particles diameter increased rather substantially with increasing of the molar ratio $[Lu^{3+}]$/urea in the reaction

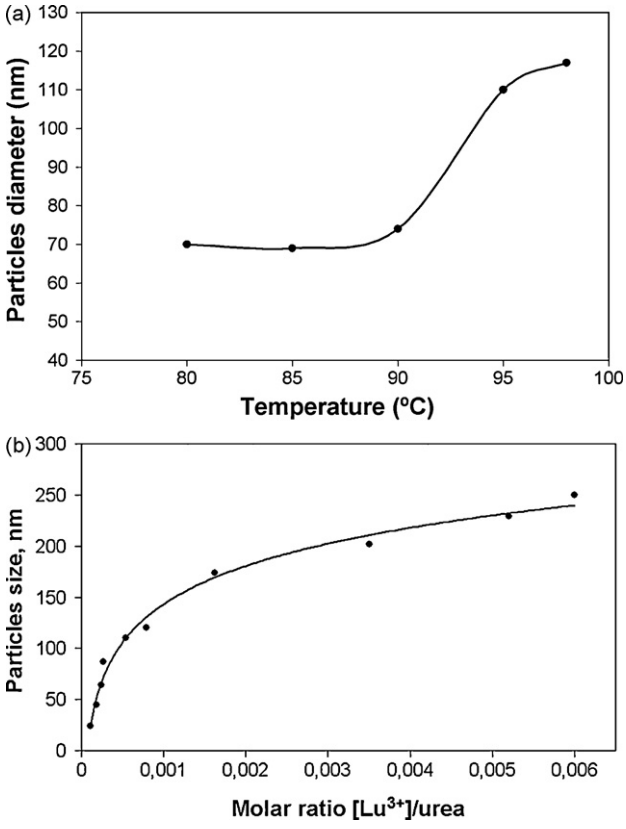

Fig. 3. Diameter of the precursor particles depending on the synthesis temperature (a) and $[Lu^{3+}]$/urea molar ratio (b).

mixture. However it should be noted that the precursor particles prepared in the high-concentration solutions of the initial reagents ($c[(NH_2)_2CO] > 3.3\ mol\ L^{-1}$; $c[Lu(NO_3)_3] > 17.4 \times 10^{-3}\ mol\ L^{-1}$) lose their spherical shape and become more aggregated by the reason of the growth in the "spatially limited" conditions. In general, the standard deviation of the size distribution of the spherical particles obtained was about ±10%. The specific surface area (BET analysis) of the Lu_2O_3:Eu^{3+} powders obtained by the urea-precipitation was ranging from 14 to 22 $m^2\ g^{-1}$ and depends on the diameter of particles and the drying conditions (Table 1). It should be

Table 1
The parameters of the Lu_2O_3:Eu^{3+} powders obtained.

Precipitant	Morphology	The average size (nm) (TEM data)	Preliminary air-drying parameters	Annealing temperature (°C)	Specific surface area (m^2/g)
NH_4OH	Agglomerated particles of the undefined shape	~15	Water, 60 °C	700	5.5
				1000	3.7
NH_4HCO_3	Agglomerated spherical-like particles	~40	Water, 60 °C	700	7.1
				1000	14.0
$(NH_2)_2CO$	Spherical	110	Water, 120 °C	700	14.4
				1000	12.5
			Water, 60 °C	700	17.0
			Water, 25 °C	700	21.6
			Ethanol, 70 °C	700	18.3
			Water, 25 °C with azeotropic dehydration	700	20.1

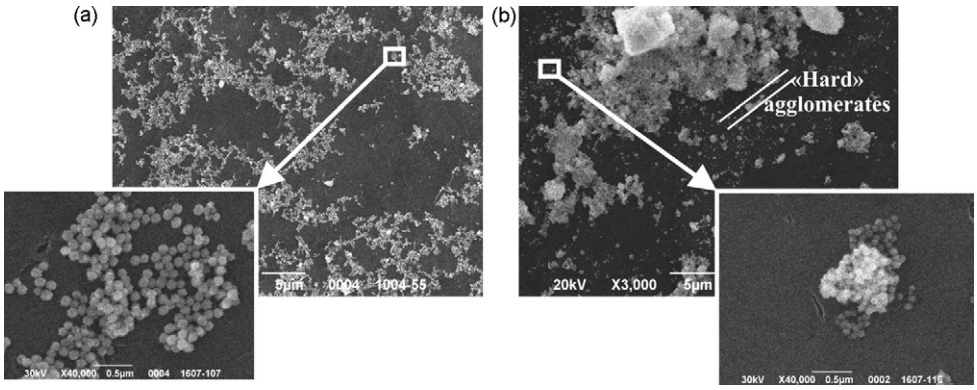

Fig. 4. SEM images of Lu_2O_3:Eu^{3+} powders dried in air at the temperatures of 25 °C (a) and 120 °C (b).

noted, that the specific surface area (SSA) values for the urea-precipitate samples are higher a little in comparison with the same values for the powder samples prepared applying NH_4OH and NH_4HCO_3 precipitants that is testifies the agglomeration processes occurred in the last ones.

The agglomeration of the particles in the highly dispersed systems is a difficult technological problem that limits the possible application of the highly dispersed powders for the creation of the close-density materials. In most cases the powder material consists of agglomerates instead of separate particles, therefore the additional treatment (surface modification, specified drying, and mechanical milling) is necessary to use for prevention of the agglomeration. The voids formed during compaction of the agglomerated powders are the main reason of the residual porosity of ceramic material. The primary agglomeration, i.e. "soft" agglomerates formation takes place in the stage of the precursor drying that result in the formation of "hard" agglomerates in the stage of high temperature annealing. Such agglomerates occur due to adhesion of the particles with high surface activity and difficultly destroyed. The comparative analysis of the SSA values of the Lu_2O_3:Eu^{3+} powder at the constant diameter of the particles allows estimating the powders agglomeration. Table 1 shows SSA values of Lu_2O_3:Eu^{3+} powders with the diameter of the particles is about 110 nm, which was exposed to the different drying methods, such as thermal and room-temperature drying in air at different temperatures from water and ethanol, and also azeotropic dehydration of the powders. It is clearly seen, that drying in air at room temperature and azeotropic distillation in the stage of dehydration allows obtaining the most non-agglomerated powder. The SEM images of Lu_2O_3:Eu^{3+} powders dried at different conditions shows the agglomerates formation after the thermal exposure (120 °C) in comparison with powders dried in air at room temperature (Fig. 4).

TG-DTA curves of the precursor powders produced by urea precipitation are given in Fig. 5. DTA shows one endothermic peak at about 190 °C, a shallow peak in the region of 320–530 °C and exothermic peak at 720 °C. The TG curve shows two steps weight loss up to 850 °C with the total weight loss is about 26%. The first endothermic peak in the DTA curve corresponds to the release of hydration water and the exothermal peak is due to the lutetium oxide crystallization. An analogical exothermal effect was observed for Y_2O_3 spherical particles crystallization.[13] On the basis of TG-DTA, IR-spectroscopy data and also reported earlier results for Y_2O_3,[13] it is possible to suggest the following mechanism of the thermal decomposition of $Lu(OH)CO_3{\cdot}H_2O$ into Lu_2O_3:

$$Lu(OH)CO_3 \cdot H_2O \xrightarrow{60-245\,^{\circ}C} \underset{(7\,wt\%)}{Lu(OH)CO_3}$$

$$\xrightarrow{245-550\,^{\circ}C} \underset{(10-18\,wt\%)}{\text{intermediate phases}} \xrightarrow{550-850\,^{\circ}C} \underset{(26\,wt\%)}{Lu_2O_3}$$

The possible intermediate phases are the carbonates and oxycarbonates lutetium, such as $Lu_2(CO_3)_3$, $Lu_2O(CO_3)_2$, and $Lu_2O_2CO_3$.[23]

Fig. 6 shows the evolution of the X-ray diffraction patterns of the undoped Lu_2O_3 spherical particles annealed in air during 2 h at temperatures 700, 900 and 1200 °C. The precursor annealed up to 700 °C was fully amorphous. All the diffraction peaks belonging to crystalline cubic Lu_2O_3 reported in the standard JCPDS card (JCPDS card 12-0728) are present in the patterns of the samples. XRD data shows that the crystallization of the spherical particles was fully complete at 700 °C, however the crystallization peak in the DTA curve registered at 720 °C (Fig. 5). Such a disagreement can be explained by the differences in the time operation of the samples. DTA analysis was carried out at dynamic heating, while before XRD analysis the samples were additionally soaked for 2 h at specified temperature. Thus

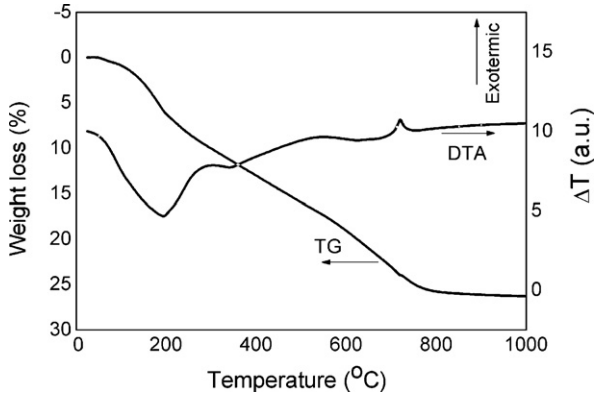

Fig. 5. TG-DTA curves of the Lu_2O_3:Eu^{3+} precursor powder dried at 60 °C.

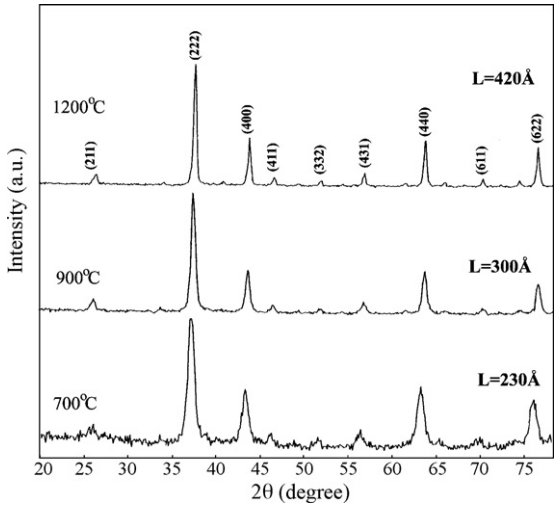

Fig. 6. X-ray diffraction patterns of the powders annealed at the specified temperatures for 2 h.

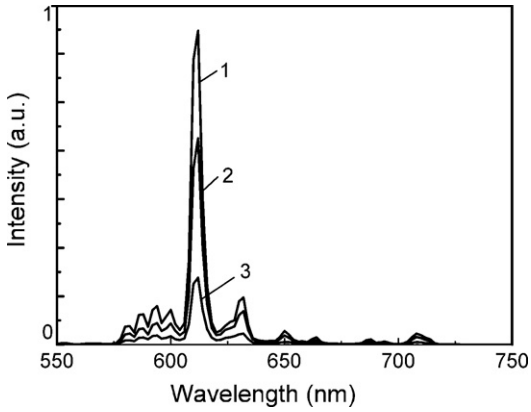

Fig. 8. Room-temperature X-ray luminescence spectra of Lu_2O_3:Eu^{3+} powders annealed at 1200 °C (1), 900 °C (2), and 700 °C (3).

the prolonged heating reduces the crystallization temperature to some extent in comparison with the thermal analysis.

The diffraction peaks become gradually narrower with the increasing of the annealing temperature, which reflects the increasing sizes (L) of the Lu_2O_3 crystallites. The average crystallite sizes calculated from the Scherrer's formula increased from 230 to 420 Å dependently on the annealing temperature (Fig. 6). The lattice parameter calculated for the undoped Lu_2O_3 powder ($a = 10.390 \pm 0.006$ Å) coincides well with the theoretical value. The increase of the lattice parameter value ($a = 10.413 \pm 0.006$ Å) of the cubic europium-doped Lu_2O_3 (Eu^{3+} – 5 at.%) was observed at the isomorphous substitution of Lu^{3+} by the bigger Eu^{3+} ion.[25]

The reduction of the particles diameter after the annealing at 900 °C is about 20% in comparison with the precursor diameter due to precursor decomposition. However, annealing at the temperature over 1000 °C results in deformation of the particles spherical shape and initiation of the sintering and agglomeration (Fig. 7).

Fig. 8 presents the luminescence spectra under X-ray excitation of the Lu_2O_3:Eu^{3+} powders obtained at different annealing temperatures. The X-ray luminescence spectra of the samples consist of group of lines in the $\lambda = 575$–725 nm spectral region

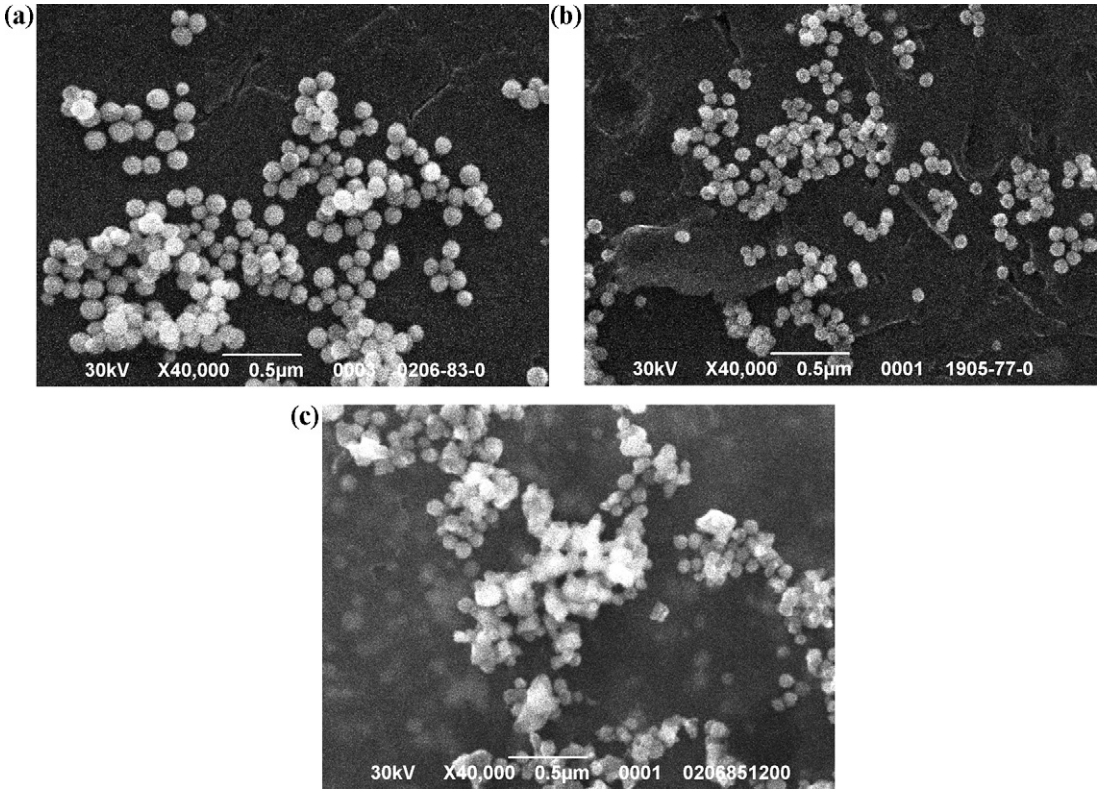

Fig. 7. SEM images of the Lu_2O_3:Eu^{3+} particles annealed at the 700 °C (a), 900 °C (b), and 1200 °C (c).

corresponding to $^5D_0 \rightarrow {}^7F_J$ transitions ($J = 0$–4) of Eu^{3+} ions and conforms well to emission of the Eu^{3+} ions in the Lu_2O_3 host lattice.[9,23] The $^5D_0 \rightarrow {}^7F_2$ electric dipole transitions with the maximum at $\lambda = 611$ nm are dominant, and the emission falls within the spectral sensitivity range of CCD camera. In the cubic Lu_2O_3 lattice two different sites are available for Eu^{3+} ions with C_2 and C_{3i} (S_6) symmetry. The Eu^{3+} ions in the C_2 non-centrosymmetric site demonstrate forced 4f–4f electric dipole transitions, while the Eu^{3+} ions in the symmetrical site of C_{3i} (S_6) are characterized only by magnetic dipole transitions with significantly lower intensity. For the Eu^{3+} ion in the S_6 site of the Lu_2O_3 host lattice it was shown that only relatively weak lines at $\lambda = 582$ nm can be registered in the luminescence spectrum.[26] Thus, the radioluminescence spectra of the Lu_2O_3:Eu^{3+} samples presented in Fig. 8 correspond to the superposition of emission of the Eu^{3+} ions occupying in Lu_2O_3 host different crystallographic positions. The high luminescence intensity of Lu_2O_3:Eu^{3+} powders under X-ray excitation evidences the presence of an efficient channel of the energy transfer from matrix to the Eu^{3+} emission centers according to a recombination mechanism.[27] The increasing of the luminescence intensity was observed with the increasing of the annealing temperature. Such luminescence increase can be explained both by the elimination of the residual OH groups in crystalline europium-doped lutetium oxide and improvement of the powders crystallinity with the rising of the annealing temperature.

Green-bodies of 70 nm Lu_2O_3:Eu^{3+} spherical particles annealed at 700 °C were formed by the cold-uniaxial pressing method. The green relative densities of the obtained compacts ranged between 38% and 52% depended on the applied pressure (Fig. 9a). At the same time, the green density of the compacts based on agglomerated Lu_2O_3:Eu^{3+} powders precipitated by the mixture NH_4OH and NH_4HCO_3 is less than 45% (pressed isostatically).[4] The compacts prepared by the cold-uniaxial pressing in this study are characterized by the relative dense random packed structures without macroscopic heterogeneities (Fig. 9b). Application of the isostatic pressing method gives the possibility of the further increase of green-body density, results in more homogeneous distribution of the density in the compacts at less quantity of internal tensions in comparison with the uniaxial pressing method. However, the processes of compactions in the mentioned above methods are too fast to allow any rearrangement, resulting in lower green density. Application of the sedimentation and slip casting methods yielded an ordered packing of particles with the density about 70%.

The densification of the Lu_2O_3:Eu^{3+} green-bodies obtained as described above with the particle size about 70 nm (Sample 1) and 150 nm (Sample 2) is displayed in Fig. 10, in terms of plots of relative shrinkage $(L_0 - L)/L_0$ (where L_0 and L are the length of the sample at the beginning and during the measurements, respectively), as a function of temperature.

The shrinkage curves are S-shaped that is typical for shrinkage of single-phase samples. Significant sintering for the Sample 1 starts at the temperature of 800 °C, which is lower for about 200 °C in comparison with the Sample 2. Shrinkage intensively decreases in the temperature range from 1000 to 1400 °C and enter to plateau for Sample 1. The shrinkage for the Sample 2

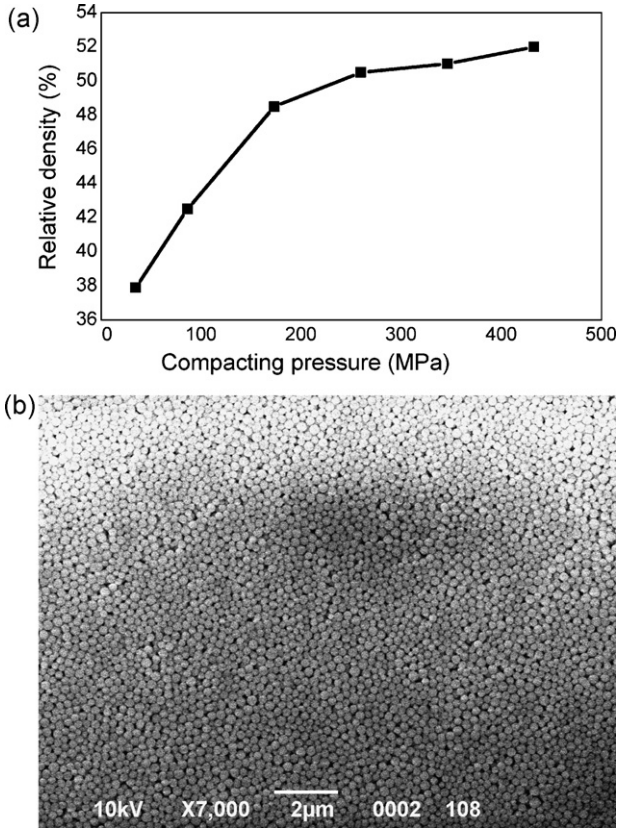

Fig. 9. The relative density of Lu_2O_3:Eu^{3+} green-bodies as a function of the applied pressure (a) and the SEM image of green-body prepared by the cold-uniaxial pressing at 440 MPa (relative density 52%) (b).

considerably less than in the case of the Sample 1 and significant sintering starts at near 1000 °C. It is known that the tendency towards agglomeration increases with the decreasing of the particles size. That is why the green density of compacts based on the 70 nm particles was lower than in the case of compacts based on 150 nm particles (45% and 38% for the Samples 2 and 1, respectively). The density after sintering was about 90% for both samples in spite of their different green densities, which can be related with the differences in the sintering processes.

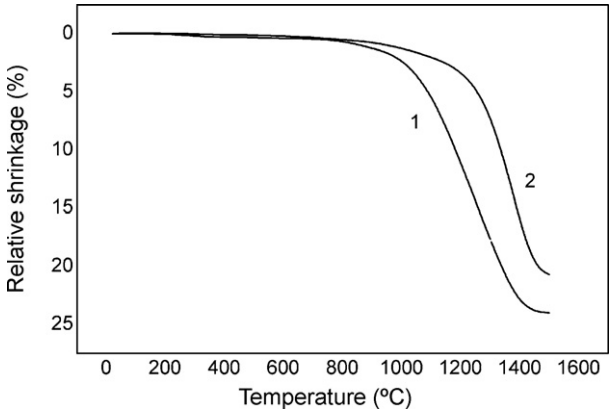

Fig. 10. Dilatometry data for Lu_2O_3:Eu^{3+} green-bodies prepared on the basis of spherical particles with the average diameter 70 nm (1) and 150 nm (2) preliminary annealed at 700 °C and pressed at 40 MPa.

A search of powders with optimum combination of spherical particles size and its sintering ability is a further task.

4. Conclusions

The non-agglomerated powders on the basis of luminescent Lu_2O_3:Eu^{3+} submicron-sized spherical particles were obtained by the urea-based homogeneous precipitation with subsequent annealing at the temperatures ranging from 700 to 1200 °C for the precursor crystallization. Combined analysis of IR and TG-DTA characterizations reveal that the precursor has a lutetium basic carbonate composition and its thermal decomposition process includes the removals of hydration water, OH^- and CO_3^{2-} ions during annealing. The diameter of the Lu_2O_3:Eu^{3+} particles obtained ranging from 50 to 250 nm (dispersion in the sizes not exceeds 10%) was controlled by the molar ratio [Lu^{3+}]/urea in the initial solutions and also the temperature of the synthesis. Lu_2O_3:Eu^{3+} cubic phase is found to crystallize at 700-720 °C and heat treatment above 1000 °C results in deformation of the spherical shape of the particles and also initiates the processes of sintering and agglomeration. The density of green-bodies obtained on the basis Lu_2O_3:Eu^{3+} powders by the cold-uniaxal pressing method was about 52% and increased up to 90% after the sintering at 1500 °C. Thus, it was shown that the Lu_2O_3:Eu^{3+} powders obtained are perspective for the close-density optical materials creation due to the high density of the spherical particles packing.

Acknowledgments

The authors are grateful to Dr. T. Korshikova, Dr. R. Yavetsky for their assistance in experimental work and discussion results.

References

1. Flores-Gonzalez MA, Louis C, Bazzi B, Ledoux G, Lebbou K, Roux S, et al. Elaboration of nanostructured Eu^{3+}-doped Gd_2O_3 phosphor fine spherical powders using polyol-mediated synthesis. *Appl Phys A* 2005;**81**:1385–91.
2. Pires AM, Santos MF, Davalos MR, Stucchi EB. The effect of Eu^{3+} doping concentration in Gd_2O_3 fine spherical particles. *J Alloys Compd* 2002;**344**:276–9.
3. Trojan-Piegza J, Zych E, Hreniak D, Strek W, Kepinski L. Structural and spectroscopic characterization of Lu_2O_3:Eu nanocrystalline spherical particles. *J Phys Condens Matter* 2004;**16**:6983–94.
4. Chen Q, Shi Y, An L, Chen J, Shi J. Fabrication and photoluminescence characteristics of Eu^{3+}-doped Lu_2O_3 transparent ceramics. *J Am Ceram Soc* 2006;**89**:2038–42.
5. Kopylov YuL, Kravchenko VB, Bagayev SN, Shemett VV, Komarov AA, Karban OV, et al. Development of Nd^{3+}:$Y_3Al_5O_{12}$ laser ceramics by high-pressure colloidal slip-casting (HPCSC) method. *Opt Mater* 2009;**31**:707–10.
6. Sun XL, Tok AIY, Huebner R, Boe FYC. Phase transformation of ultrafine rare earth oxide powders synthesized by radio frequency plasma spraying. *J Eur Ceram Soc* 2007;**17**:125–30.
7. Somiya Sh, Roy R. Hydrothermal synthesis of fine oxide powders. *Bull Mater Sci* 2000;**23**:453–60.
8. Cabrera AF, Mudarra Navarro AM, Rodrıguez Torres CE, Sanchez FH. Mechanosynthesis of Fe-doped SnO_2 nanoparticles. *Physica B* 2007;**398**:215–8.
9. Zych E, Hreniak D, Strek W. Spectroscopy of Eu-doped Lu_2O_3-based X-ray phosphor. *J Alloys Compd* 2002;**341**:385–90.
10. Trojan-Piegza J, Zych E. Preparation of nanocrystalline Lu_2O_3:Eu phosphor via a molten salt route. *J Alloys Compd* 2004;**380**:118–22.
11. Lu J, Lu J, Murai T, Takaichi K, Uematsu T, Ueda K, et al. Nd^{3+}:Y_2O_3 ceramic laser. *J Appl Phys* 2001;**40**:1277–9.
12. Ikegami T, Li J-G, Mori T, Moriyoshi Y. Fabrication of transparent yttria ceramics by the low-temperature synthesis of yttrium hydroxide. *J Am Ceram Soc* 2002;**85**:1725–9.
13. Aiken B, Hsu WP, Matijevik E. Preparation and properties of monodispersed colloidal particles of lanthanide compounds: III, yttrium(III) and mixed yttrium(III)/cerium(III) systems. *J Am Ceram Soc* 1988;**71**:845–53.
14. Li J-G, Li X, Sun X, Ikegami T, Ishigaki T. Uniform colloidal spheres for $(Y_{1-x}Gd_x)_2O_3$ (x = 0–1): formation mechanism, compositional impacts, and physicochemical properties of the oxides. *Chem Mater* 2008;**20**:2274–81.
15. Sanada T, Kawai M, Nakashita H, Matsumoto T, Wada N, Kojima K. Preparatoin of undoped and Tb^{3+}-doped fluorescent HfO_2 spherical particles. *J Ceram Soc Jpn* 2008;**116**:1265–9.
16. Mouzon J. Influence of agglomeration on the transparency of yttria ceramics. *J Am Ceram Soc* 2008;**91**:3380–7.
17. Peters R, Kränkel C, Petermann K, Huber G. Broadly tunable high-power Yb:Lu_2O_3 thin disk laser with 80% slope efficiency. *Opt Exp* 2007;**15**:7075–82.
18. Lu J, Takaichi K, Uematsu T, Shirakawa A, Musha M, Ueda K, et al. Promising ceramic laser material: highly transparent Nd^{3+}:Lu_2O_3 ceramic. *Appl Phys Lett* 2002;**81**:4324–6.
19. Lempicki A, Brecher C, Szupryczynski P, Lingertat H, Nagarkar VV, Tipnis SV, et al. A new lutetia-based ceramic scintillator for X-ray imaging. *NIM A* 2002;**488**:579–90.
20. Boyer JC, Vetrone F, Capobianco JA, Speghini A, Bettinelli M. Variation of fluorescence lifetimes and judd-ofelt parameters between Eu^{3+} doped bulk and nanocrystalline cubic Lu_2O_3. *J Phys Chem* 2004;**108**:20137–43.
21. Shi Y, Chen QW, Shi JL. Processing and scintillation properties of Eu^{3+} doped Lu_2O_3 transparent ceramics. *Opt Mater* 2008;**31**:729–33.
22. Wang Z, Zhang W, Lin L, You B, Fu Yi, Yin M. Preparation and spectroscopic characterization of Lu_2O_3:Eu^{3+} nanopowders and ceramics. *Opt Mater* 2008;**30**:1484–8.
23. Chen Q, Shi Y, An L, Wang S, Chen J, Shi J. A novel co-precipitation synthesis of a new phosphor Lu_2O_3:Eu^{3+}. *J Eur Ceram Soc* 2007;**27**:191–7.
24. Kaliszewski MS, Heuer AH. Alcohol interaction with zirconia powders. *J Am Ceram Soc* 1990;**73**:1504–9.
25. Shannon R. Revised effective ionic radii and systematic studies of interatomic distances in halides and chalcogenides. *Acta Crystallogr A* 1979;**32**:751–67.
26. Zych E. Concentration dependence of energy transfer between Eu^{3+} ions occupying two symmetry sites in Lu_2O_3. *J Phys Condens Matter* 2002;**14**:5637–50.
27. Zych E, Trojan-Piegza J. Low-temperature luminescence of Lu_2O_3:Eu ceramics upon excitation with synchrotron radiation in the vicinity of band gap energy. *Chem Mater* 2006;**18**:2194–9.